SIAM J. APPL. MATH.
Vol. 67, No. 3, pp. 757–776

ANALYSIS OF A MODEL OF THE GLUCOSE-INSULIN REGULATORY SYSTEM WITH TWO DELAYS*

JIAXU LI† AND YANG KUANG‡

Abstract. We continue a recent attempt to better understand the glucose-insulin regulatory system via a mathematical model of delay differential equations with two discrete time delays. With explicit delays, the model is more realistic in physiology, more accurate in mathematics, and more robust in applications. We study this model analytically and perform carefully designed numerical simulations by allowing two parameters to vary. Our analytical and numerical results confirm most current existing physiological observations and reveal more insightful information. The following factors are critical for ensuring the sustained oscillatory regulation and insulin secretion: (1) the time lag for insulin secretion stimulated by glucose and the newly synthesized insulin becoming *"remote insulin"* (Theorem 4.2 (b) and Theorem 5.6); (2) the delayed effect of hepatic glucose production (Theorem 4.2 (c) and Theorem 5.6); (3) moderate insulin clearance rate (Theorem 5.6 and simulations in section 6.4); and (4) nonoverwhelming glucose infusion (simulations in section 6.2, 6.3, and 6.4).

Key words. glucose-insulin regulatory system, insulin secretion, ultradian oscillation, time delay

AMS subject classifications. 92C50, 34C60, 92D25

DOI. 10.1137/050634001

1. Introduction.

Beginning with the pioneering work of Bolie [5] in the 1960s, several attempts at modeling the glucose-insulin regulatory system have been proposed in recent decades [2], [17], [25], [26]. These studies are, at least partially, motivated by the fact that diabetes mellitus is one of the worst diseases in the world due to the large size of the diabetic population, especially among Native Americans [14], as well as severe complications [10] and high health expenses (http://www.diabetes.org). Providing more efficient, effective, and economic treatments is the ultimate goal of these efforts (see [2], [3], [4], [5], [17], [18], [25], [26], and the references therein). The minimal model [3] and its siblings [9], [16], [19] study the insulin sensitivity, while the mathematical models proposed in [2], [5], [17], [25], [26] aim to better understand the glucose-insulin regulatory system.

In the glucose-insulin endocrine metabolic regulatory system, the pancreatic hormone insulin and glucagon are the two key players. Both in-vivo and in-vitro experiments have revealed that the insulin is secreted from the pancreas in oscillatory manners in two time scales. It is widely believed that the rapid pulsatile oscillation is caused by the insulin secretory bursts from the millions of Langerhans islets in hundreds of β-cells in the pancreas at a periodicity of 5–15 minutes [20]. The much slower ultradian oscillation refers to the oscillation of insulin secretion with period in the range of 50–150 minutes [23], [25]. The amplitude of the ultradian oscillation dominates that of the rapid pulsatile oscillation. There exist two time delays in this

*Received by the editors June 19, 2005; accepted for publication (in revised form) November 2, 2006; published electronically March 15, 2007.
http://www.siam.org/journals/siap/67-3/63400.html
†Department of Mathematics and Statistics, Arizona State University, Tempe, AZ 85287-1804 (jiaxu.li@asu.edu). Current address: Department of Mathematics, University of Louisville, Louisville, KY 40929. The work of this author was partially supported by ASU grant MGIA-2006-08.
‡Department of Mathematics and Statistics, Arizona State University, Tempe, AZ 85287-1804 (kuang@asu.edu). The work of this author was partially supported by grants DMS-0077790 and DMS/NIGMS-0342388 and ASU grant MGIA-2006-08.

system. One naturally occurring time delay is the time needed for the insulin to release from the β-cells stimulated by elevated glucose concentration and the newly synthesized insulin to cross the endothelial barriers and become the so-called *remote insulin*, now known as interstitial insulin. The remote insulin helps the cells, e.g., muscle and adipose, to uptake glucose. The other time delay refers to the delayed effect of hepatic glucose production. Applying the standard compartment transition technique to mimic the time delays, Sturis et al. [25] formulated a model consisting of six ordinary differential equations (ODEs) that successfully captured some of the basic features (oscillations with periods and amplitudes comparable to experiment observations) of ultradian oscillation. Recently, Li, Kuang, and Mason [17] proposed an alternative model of the glucose-insulin regulatory system consisting of two delay differential equations with two naturally explicit discrete time delays. This two-delay model uses only physiologically meaningful and measurable parameters. It is shown that this two-delay model provides the best overall fit among five plausible model systems with the experimental data given in [2], [17], and [25]. It is also shown [17] that the two-time-delay model is more robust compared to the model proposed in [25]. The authors of [17] concluded that the time delay of insulin responding to glucose stimulation plays a key role in generating the oscillatory behavior of insulin secretion.

This paper attempts to provide a systematical study of the two-delay model of [17] with focuses on analytical studies, bifurcation analysis, and carefully designed numerical simulations. In the following sections, we first introduce the model proposed in [17], then present some preliminary results on positivity, boundedness, and persistence of solutions. Local stability analyses are carried out in details whenever feasible. These analytical results are complemented and confirmed by the bifurcation diagrams produced from our extensive and carefully designed simulations. This paper ends with a discussion section containing a list of observations.

2. The two-delay model. By applying the mass conservation law, the approach used in [27], Li, Kuang, and Mason [17] proposed a glucose-insulin regulatory system model with two explicit time delays based on a set of well-known observations [1], [6], [13], [17], [21], [25], [26], [27]. The model can be expressed by the following word equations.

Glucose change rate = glucose production rate − glucose utilization rate.
Insulin change rate = insulin production rate − insulin removal rate.

Throughout this paper, we use $G(t)$ to represent the plasma glucose concentration and $I(t)$ to represent the plasma insulin concentration at time $t \geq 0$.

In the glucose-insulin endocrine metabolic system, the β-cells, contained in the Langerhans islets in the pancreas, are the only source of insulin production. When the plasma glucose concentration level is elevated, the β-cells secrete insulin after a complex series of cascading physiological processes [1], [17]. The newly synthesized insulin crosses the endothelial barriers to become remote insulin, which readily helps the cells, e.g., muscle and fat cells, to utilize the plasma glucose and convert it to energy [17]. These processes take a total of approximately 5–15 minutes [25], [26]. In the model, this is denoted by $f_1(G(t-\tau_1))$, where $\tau_1 > 0$ represents the time delay of the insulin response to the glucose stimulation and the time needed for the newly synthesized insulin crossing endothelial barrier to become remote insulin.

Insulin is degraded by all insulin sensitive tissues, and the degradation is mediated primarily by the insulin receptor with a smaller contribution from nonspecific

processes. The liver and kidney are the primary sites of portal insulin degradation and peripheral insulin clearance, respectively. Insulin not cleared by the liver and kidneys is ultimately removed mainly by muscle and adipose cells [11], [17]. The function of insulin clearance is to remove and inactivate circulating insulin in order to control insulin action [11]. The degradation is almost linearly proportional to insulin [27]. So the degradation rate is denoted by a constant $d_i > 0$. Since $I(t)$ stands for plasma insulin concentration, it is easier to measure clinically.

In muscle and adipose tissue, insulin facilitates the transport of glucose into cells. The glucose is then metabolized by the cells. This type of glucose consumption is called insulin-dependent glucose utilization. Not all glucose consumption depends on the attendance of insulin. For example, the brain and nerve cells consume the glucose without the aid of insulin. This is referred to as insulin-independent glucose utilization. (See [17] for more details.) Respectively, the insulin-independent and insulin-dependent glucose utilization are represented by $f_2(G(t))$ and $f_3(G(t))f_4(I(t))$.

Glucose enters the circulation in two ways: glucose infusion and hepatic glucose production. Glucose infusion includes meal ingestion, oral glucose intake, continuous enteral nutrition absorption, and constant infusion. Hence the model includes a constant glucose infusion term G_{in} that may model the continuous enteral glucose absorption and constant glucose infusion [17], [25], [27].

Hepatic glucose production is due to glucose dispensation by the liver endogenously. When the plasma glucose concentration level becomes low, the β-cells stop releasing insulin. Instead, the α-cells, also contained in Langerhans islets, start to release glucagon. Glucagon exerts control over pivotal metabolic pathways in the liver and leads the liver to dispense glucose [1]. The liver also converts the previously stored glycogen into glucose. Opposite to the fact that glucagon secretion triggers the liver to dispense glucose, insulin secretion inhibits glucose production by the liver [6], [21]. Thus the hepatic glucose production is primarily controlled by insulin concentration in both inhibitory effect by insulin secretion and recovery effect by insulin suppression. Some time is needed for hepatic glucose production to take significant effect, e.g., half maximal suppression or recovery takes time [17], [21]. However, both the pathways and the length of the delay remain unknown. Nevertheless, this time delay is approximately between a few minutes and a half hour, or even longer [17], [21]. The hepatic glucose production is presented by $f_5(I(t-\tau_2))$, where $\tau_2 > 0$ represents the time taken for a noticeable effect on hepatic glucose production, e.g., half maximal suppression or recovery rate.

Therefore the system [17] can be written as

$$\begin{cases} G'(t) = G_{in} - f_2(G(t)) - f_3(G(t))f_4(I(t)) + f_5(I(t-\tau_2)), \\ I'(t) = f_1(G(t-\tau_1)) - d_i I(t). \end{cases} \tag{2.1}$$

For convenience, the initial conditions of the two-time-delay model (2.1) are assumed to be $I(0) = I_0 > 0$, $G(0) = G_0 > 0, G(t) \equiv G_0$ for all $t \in [-\tau_1, 0]$ and $I(t) \equiv I_0$ for $t \in [-\tau_2, 0]$, $\tau_1, \tau_2 > 0$. In this paper, we assume that the functions f_i, $i = 1, 2, 3, 4, 5$, in model (2.1) satisfy the following conditions:

(i) Notice that β-cells release insulin due to glucose stimulation. We assume that $f_1(x) > 0$ and $f_1'(x) > 0$ for $x > 0$. On the other hand, the capacity of the insulin secretion from β-cells is saturated due to highly increased glucose concentration level, so we assume $\lim_{x\to\infty} f_1(x) = M_1$ and $f_1'(x)$ is bounded by a constant $M_1' > 0$ for $x > 0$. Thus it is reasonable to assume that $f_1(x)$ is in sigmoidal shape. Observing that the insulin can be secreted from the β-cells due to bursting without the glucose stimulation, we assume that $f_1(0) := m_1 > 0$.

(ii) As a term indicating the insulin-independent glucose utilization, it is clear that $f_2(0) = 0$, $f_2(x) > 0$, and $f_2'(x) > 0$ for $x > 0$. On the other hand, the utilization is not unlimited, so we assume that $\lim_{x\to\infty} f_2(x) = M_2$ and there exists a constant M_2' such that $f_2'(x) < M_2'$ for $x > 0$.

(iii) The insulin-dependent glucose utilization $f_3(G(t))f_4(I(t))$ can be depicted as $f_3(0) = 0$, $f_4(0) := m_4 > 0$, $f_3'(x) > 0$, $f_4(x) > 0$, and $f_4'(x) > 0$ for $x > 0$. As suggested by Sturis et al. [25], we also assume that there exist constants $k_3 > 0, M_4 > 0$, and $M_4' > 0$ such that $0 < f_3(x) \le k_3 x$, $\lim_{x\to\infty} f_4(x) = M_4$, and $f_4'(x) < M_4'$ for $x > 0$ and $f_4(x)$ is in sigmoidal shape.

(iv) Low glucose concentration will lead β-cells to stop releasing insulin and α-cells to release glucagon. Thus, when insulin is deficit, liver dispenses glucose caused by glucagon exerting control over pivotal metabolic pathways in the liver, and also converts glycogen into glucose. On the other hand, the liver stops this process when insulin is abundant. Hence we assume $f_5(0) > 0$, $f_5(x) > 0$, and $f_5'(x) < 0$ for $x > 0$, and $\lim_{x\to\infty} f_5(x) = 0$ and f_5 is in inverse sigmoidal shape. Since the amount of glucose converted by the liver is small and the process takes time, we assume $\exists M_5, M_5' > 0$ such that $f_5(x) \le M_5$ and $|f_5'(x)| \le M_5'$ for $x > 0$. We can simply set $M_5 = f_5(0)$.

The shapes of the functions are more important than their forms [13]. Figure 3 of [17] shows the shapes of functions in model (2.1). In section 6, we adopt the functions, (6.1)–(6.5), used in [17], [25], and [26], to perform numerical simulations.

3. Preliminaries. We first present some useful preliminary results of model (2.1). The following fluctuation lemma is elementary and well known [12].

LEMMA 3.1 (fluctuation lemma). *Let $f : \mathbf{R} \to \mathbf{R}$ be a differentiable function. If $l = \liminf_{t\to\infty} f(t) < \limsup_{t\to\infty} f(t) = L$, then there are sequences $\{t_k\} \uparrow \infty$, $\{s_k\} \uparrow \infty$ such that for all k, $f'(t_k) = f'(s_k) = 0, \lim_{k\to\infty} f(t_k) = L$, and $\lim_{k\to\infty} f(s_k) = l$.*

We will apply Lemma 3.1 in the proofs of Proposition 3.2 on solution boundedness and Lemma 3.3 on a set of restrictions for the upper and lower limits of a solution. The proofs are given in Appendices A and B.

PROPOSITION 3.2. *In model (2.1), the following hold:*

(i) *If $\lim_{x\to\infty} f_3(x) > (G_{in} - M_2 + M_5)/m_4$, then model (2.1) has unique positive steady state (G^*, I^*) with $I^* = d_i^{-1} f_1(G^*)$. Furthermore, all solutions exist in $(0, \infty)$, and are positive and bounded.*

(ii) *If $\lim_{x\to\infty} f_3(x) < (G_{in} - M_2)/m_4$, then $\limsup_{t\to\infty} G(t) = \infty$.*

Remark. Condition (i) indicates that the steady state is unique if insulin can help the cells to metabolize enough glucose. Otherwise, if condition (ii) holds, the glucose concentration level will be unbounded.

Remark. If $f_3(x) = k_3 x$, where $k_3 > 0$ is a constant, then

$$\limsup_{t\to\infty} G(t) \le M_G := (G_{in} + M_5)/(m_4 k_3). \tag{3.1}$$

In fact, notice that $m_4 \le f_4(x) \le M_4$ and $f_5(x) \le M_5$ and $f_3(x) = k_3 x$ for $x > 0$. Thus $G'(t) = G_{in} - f_2(G(t)) - f_3(G(t))f_4(I(t)) + f_5(I(t-\tau_2)) \le G_{in} - m_4 k_3 G(t) + M_5$. A standard comparison argument yields (3.1).

Throughout this paper, we assume that condition (i) in Proposition 3.2 holds.

Let $(G(t), I(t))$ be a solution of (2.1). Throughout this paper, we denote

$$\overline{G} = \limsup_{t\to\infty} G(t), \qquad \underline{G} = \liminf_{t\to\infty} G(t), \qquad \overline{I} = \limsup_{t\to\infty} I(t), \qquad \underline{I} = \liminf_{t\to\infty} I(t).$$

Due to Proposition 3.2, it is clear that these limits are finite. Further, we have the following lemma.

LEMMA 3.3. *If* $(G(t), I(t))$ *is a solution of* (2.1)*, then*

$$f_1(\underline{G}) \le d_i \underline{I} \le d_i \bar{I} \le f_1(\bar{G}), \tag{3.2}$$

$$f_2(\bar{G}) + f_3(\bar{G}) f_4(\underline{I}) \le G_{in} + f_5(\underline{I}), \tag{3.3}$$

$$G_{in} + f_5(\bar{I}) \le f_2(\underline{G}) + f_3(\underline{G}) f_4(\bar{I}). \tag{3.4}$$

Remark. Apparently, $\bar{G} = \underline{G}$ implies $\bar{I} = \underline{I}$ due to (3.2). If $\bar{I} = \underline{I}$, then (3.3) and (3.4) together lead to $f_2(\bar{G}) - f_2(\underline{G}) \le f_4(\bar{I})(f_3(\underline{G}) - f_3(\bar{G})) \le 0$. That is, $\bar{G} = \underline{G}$.

PROPOSITION 3.4. *Model* (2.1) *is persistent, that is, the components of all solutions are eventually uniformly bounded from above and away from zero.*

Proof. Notice that $f_2(0) + f_3(0) = 0$ and $f_4(x) < M_4$ for all $x \ge 0$. Then (3.4) implies that $G_{in} \le f_2(\underline{G}) + f_3(\underline{G}) M_4$ for all $t > 0$. Thus $\exists \delta_G > 0, t_G > 0$, such that $G(t) > \delta_G$ for $t > t_G > 0$. Hence $G(t)$ is eventually and uniformly bounded away from zero. Inequality (3.2) implies the same for $I(t)$. The parts of boundedness from above are implied in Proposition 3.2. ∎

4. Local analysis: Case $\tau_1\tau_2 = 0$. We analyze the trivial case $\tau_1\tau_2 = 0$ in this section. The study of the nontrivial case $\tau_1\tau_2 > 0$ will be carried out in the next section.

Clearly the linearized system of model (2.1) about (G^*, I^*) is given by

$$\begin{cases} G'(t) = -AG(t) - BI(t) - CI(t - \tau_2), \\ I'(t) = DG(t - \tau_1) - d_i I_1(t), \end{cases} \tag{4.1}$$

where

$$\begin{cases} A := f_2'(G^*) + f_3'(G^*) f_4(I^*) > 0, \ B := f_3(G^*) f_4'(I^*) > 0, \\ C := -f_5'(I^*) > 0, \ D := f_1'(G^*) > 0. \end{cases} \tag{4.2}$$

The characteristic equation of (4.1) is given by

$$\Delta(\lambda) = \lambda^2 + (A + d_i)\lambda + d_i A + DBe^{-\lambda\tau_1} + DCe^{-\lambda(\tau_1+\tau_2)} = 0. \tag{4.3}$$

Notice that $\Delta(0) = d_i A + DB + DC > 0$. So $\lambda = 0$ is not a solution of the characteristic equation (4.3). Thus, if there is any stability switch of the trivial solution of the linearized system (4.1), there must exist a pair of pure conjugate imaginary roots of the characteristic equation (4.3).

When $\tau_1 = \tau_2 = 0$, the original model (2.1) is an ODE model. The characteristic equation of its linearized equation is given by

$$\Delta(\lambda) = \lambda^2 + (A + d_i)\lambda + d_i A + DB + DC = 0.$$

Then, $A + d_i > 0$ and $d_i A + DB + DC > 0$ imply that (G^*, I^*) is stable.

For the cases of $\tau_1\tau_2 = 0$ and $\tau_1 + \tau_2 > 0$, we need the following lemma, which can be obtained via a standard imaginary root crossing method [8], [15]. The details can be found in [15, pp. 74–77] and [15, Theorem 3.1].

LEMMA 4.1. *Assume* $a, c, d > 0$ *in the following delay differential equation:*

$$x''(t) + ax'(t) + cx(t) + dx(t - \tau) = 0, \ \tau \ge 0. \tag{4.4}$$

Then the number of pairs of pure imaginary roots of the characteristic equation

$$\lambda^2 + a\lambda + c + de^{-\lambda\tau} = 0, \ \tau \ge 0, \tag{4.5}$$

can be zero, one, or two only.

(i) *If* $c > d$ *and* $2c - a^2 < 2\sqrt{c^2 - d^2}$, *then the number of such roots is zero for* $\tau > 0$. *The trivial solution of* (4.4) *is stable for all* $\tau > 0$.

(ii) *If* $c < d$ *or* $d = c$ *and* $2c - a^2 > 0$, *then the number of such roots is one for some* $\tau > 0$. *The trivial solution of* (4.4) *is uniformly asymptotically stable for* $\tau < \tau_0$, *and it becomes unstable for* $\tau > \tau_0$, *where* $\tau_0 > 0$ *is a constant. It undergoes a supercritical Hopf bifurcation at* $\tau = \tau_0$.

(iii) *If* $c > d$ *and* $2c - a^2 > 2\sqrt{c^2 - d^2}$, *then the number of such roots is two for some* $\tau > 0$. *The stability of the trivial solution of* (4.4) *can change (when changing from stable to unstable, the trivial solution undergoes a supercritical Hopf bifurcation) a finite number of times at most as* τ *increases, and eventually it becomes unstable.*

For the case of $\tau_1 > 0$ and $\tau_2 = 0$, the characteristic equation is

$$\Delta(\lambda) = \lambda^2 + (A + d_i)\lambda + d_i A + (DB + DC)e^{-\lambda\tau_1} = 0. \tag{4.6}$$

Notice that, in this case, $2c - a^2 = -A^2 - d_i^2 < 0$ in Lemma 4.1. Then $d_i A > D(B + C)$ implies that the trivial solution of (4.1) is always stable for $\tau_1 > 0$. Also, $d_i A < D(B + C)$ implies that $\exists \tau_{10} > 0$ such that the trivial solution of the linearized system (4.1) is stable when $\tau_1 \in (0, \tau_{10})$ and unstable when $\tau_1 \geq \tau_{10}$.

For the case of $\tau_1 = 0$ and $\tau_2 > 0$, the characteristic equation becomes

$$\Delta(\lambda) = \lambda^2 + (A + d_i)\lambda + (d_i A + DB) + DCe^{-\lambda\tau_2} = 0. \tag{4.7}$$

In Lemma 4.1, $2c - a^2 = 2DB - A^2 - d_i^2$. Thus if $d_i^2 > 2DB - A^2$ and $d_i A > D(C - B)$, the trivial solution of (4.1) is stable for all $\tau_2 > 0$. If $d_i A < D(C - B)$, then the stability of the trivial solution of (4.1) switches from stable to unstable when τ_2 increases through a critical value $\tau_{20} > 0$ and remains unstable for $\tau_2 > \tau_{20}$. If $d_i A > D(C - B)$ and $2DB - A^2 - d_i^2 > 2\sqrt{(d_i A + DB)^2 - D^2C^2}$, then the trivial solution of the linearized system (4.1) has at most a finite number of stability switches and eventually is unstable.

Define

$$H_1(d_i, G_{in}) = D(B + C) - d_i A. \tag{4.8}$$

We summarize the above analysis in the following theorem for model (2.1).

THEOREM 4.2. *Consider model* (2.1).

(a) *If* $\tau_1 = 0$ *and* $\tau_2 = 0$, *then* (G^*, I^*) *is stable.*

(b) *If* $\tau_1 > 0$ *and* $\tau_2 = 0$, *and*

(b.1) *if* $H_1(d_i, G_{in}) < 0$, *then* (G^*, I^*) *is stable for* $\tau_1 > 0$;

(b.2) *if* $H_1(d_i, G_{in}) > 0$, *then* $\exists \tau_{10} > 0$ *such that* (G^*, I^*) *is stable when* $\tau_1 \in (0, \tau_{10})$ *and unstable when* $\tau_1 \geq \tau_{10}$.

(c) *When* $\tau_1 = 0$ *and* $\tau_2 > 0$,

(c.1) *if* $D(C - B) - d_i A < 0$ *and* $d_i^2 > 2DB - A^2$, *then* (G^*, I^*) *is stable;*

(c.2) *if* $D(C - B) - d_i A > 0$, *then* $\exists \tau_{20} > 0$ *such that* (G^*, I^*) *is stable when* $\tau_2 \in (0, \tau_{20})$ *and unstable when* $\tau_1 \geq \tau_{20}$;

(c.3) *if* $D(C - B) - d_i A < 0$ *and* $2DB - A^2 - d_i^2 > 2\sqrt{(d_i A + DB)^2 - D^2C^2}$, *then there are at most a finite number of stability switches and eventually* (G^*, I^*) *is unstable,*

where A, B, C, *and* D *are given in* (4.2).

With the specific functions (6.1)–(6.5) in section 6, Figure 5.1 (right) demonstrates the curve $H_1(d_i, G_{in}) = 0$ in the (G_{in}, d_i)-plane. The curves in Figure 5.1 (right) are

independent of delay τ_1 and τ_2. The steady state is stable when $(G_{in}, d_i) \in R_s$, that is, d_i is small. Our computations show that conditions (b.1) and (c.3) in Theorem 4.2 do not hold. Condition (c.1) holds for some values (G_{in}, d_i), and thus the sustained oscillations would not occur.

When condition (b.2) ($\tau_2 = 0$) or (c.2) ($\tau_1 = 0$) holds, the sustained oscillation takes place if $\tau_1 > \tau_{10}$ or $\tau_2 > \tau_{20}$. Based on the arguments (3.12)–(3.17) from [15, pp. 74–76], we have

$$\tau_{10} = \theta_1/\omega_{1+},$$

where ω_{1+} is the root of (4.6) given by

$$\omega_{1+}^2 = \frac{1}{2}\Big\{ -(A^2 + d_i^2) + \Big[(A^2 - d_i^2)^2 + 4D^2(B + C)^2\Big]^{-\frac{1}{2}}\Big\},$$

and $0 \le \theta_1 < 2\pi$, satisfying

$$\begin{cases} \cos\theta_1 = (\omega_{1+}^2 - d_i A)/(DB + DC), \\ \sin\theta_1 = \omega_{1+}(A + d_i)/(DB + DC). \end{cases}$$

Similarly, we have

$$\tau_{20} = \theta_2/\omega_{2+},$$

where ω_{2+} is the root of (4.7) given by

$$\omega_{2+}^2 = \frac{1}{2}\Big\{2DB - (A^2 + di^2) + \Big[(A^2 - d_i^2)^2 - 4DB(A + d_i)^2 + 4D^2C^2\Big]^{-\frac{1}{2}}\Big\},$$

and $0 \le \theta_1 < 2\pi$, satisfying

$$\begin{cases} \cos\theta_2 = (\omega_{2+}^2 - d_i A - DB)/(DC), \\ \sin\theta_2 = \omega_{2+}(A + d_i)/(DC). \end{cases}$$

When condition (b.2) ($\tau_2 = 0$) holds, our computations show that no sustained oscillation occurs when $\tau_1 < 9$. Similarly, when (c.2) ($\tau_1 = 0$) holds, $\tau_{20} > 12$ for $G_{in} < 0.15$ or $G_{in} > 0.85$, and $d_i = 0.06$. Specifically, if $G_{in} = 1.35, d_i = 0.06$, then the Hopf bifurcation point $\tau_{20} > 40$. These observations, with Theorem 4.2 (a), suggest that both delay τ_1 and τ_2 are critical for sustained oscillations in physiologically meaningful ranges. In addition, notice that condition (b.2) automatically holds if (c.2) holds. This seems to suggest that the role of delay τ_1 is more critical than the role of delay τ_2 to ensure the sustained oscillations of the glucose-insulin regulatory system.

5. Local analysis: Case $\tau_1\tau_2 > 0$. Now assume both $\tau_1 > 0$ and $\tau_2 > 0$. Let $\lambda = \omega i$, $\omega > 0$, be such an eigenvalue in (4.3); then we have

$$\begin{aligned}\Delta(\omega i) = {} & [-\omega^2 + d_i A + DB\cos\omega\tau_1 + DC\cos\omega(\tau_1 + \tau_2)] \\ & + i[(A + d_i)\omega - DB\sin\omega\tau_1 - DC\sin\omega(\tau_1 + \tau_2)] = 0.\end{aligned}$$

That is,

$$\begin{cases} -\omega^2 + d_i A + DB\cos\omega\tau_1 + DC\cos\omega(\tau_1 + \tau_2) = 0, \\ (A + d_i)\omega - DB\sin\omega\tau_1 - DC\sin\omega(\tau_1 + \tau_2) = 0. \end{cases} \tag{5.1}$$

This leads to

$$\omega^4 + (A^2 + d_i^2)\omega^2 + d_i^2 A^2 = D^2(B^2 + C^2 + 2BC\cos\omega\tau_2). \tag{5.2}$$

5.1. Stability of the steady state. We shall consider the stability of the steady state first. From (5.2),

$$\omega^4 + (A^2 + d_i^2)\omega^2 + d_i^2 A^2 \le D^2(B^2 + C^2 + 2BC) = D^2(B + C)^2.$$

It is impossible if $d_i A \ge D(B + C)$. So, by definition of $H_1(G_{in}, d_i)$ in (4.8), we have the following proposition.

PROPOSITION 5.1. *In the linearized system* (4.1)*, when* $\tau_1 > 0$ *and* $\tau_2 > 0$*, if* $H_1(G_{in}, d_i) \le 0$*, then the steady state of the linearized system* (4.1) *is stable.*

Therefore we have the following theorem.

THEOREM 5.2. *In model* (2.1)*, if* $\tau_1 > 0$*,* $\tau_2 > 0$ *and*

$$H_1(d_i, G_{in}) = D(B + C) - d_i A \le 0, \tag{5.3}$$

then the steady state (G^*, I^*) *of system* (2.1) *is stable.*

Remark. When $\tau_1 > 0$, the same condition $H_1(d_i, G_{in}) = D(B + C) - d_i A < 0$ ensures the steady state of system (2.1) to be stable regardless of whether $\tau_2 = 0$ or $\tau_2 > 0$.

5.2. Instability of the steady state. We now study the instability of the steady state (G^*, I^*). We will apply *Rouchè's theorem* [7, pp. 125–126] to identify the case that the characteristic equation (4.3) has roots with positive real part.

ROUCHÈ'S THEOREM. *Given two functions* $f(z)$ *and* $g(z)$ *analytic in a simple connected region* $\mathcal{A} \subset \mathbf{C}$ *with boundary* γ*, a simple loop homotopic to a point in* $\mathcal{A}$*, if* $|f(z)| > |g(z)|$ *on* γ*, then* $f(z)$ *and* $f(z) + g(z)$ *have the same number of zeros in* $\mathcal{A}$*.*

Let

$$S_1 = \left\{ \frac{2m}{2n-1} : m, n \in \mathbf{Z}^+, m, n \ge 1 \right\} \text{ and } S_2 = \left\{ \frac{2m-1}{2n} : m, n \in \mathbf{Z}^+, m, n \ge 1 \right\}.$$

Clearly $\mathbf{Q}^+ = S_1 \cup S_2$ and $S_1 \cap S_2 = \emptyset$. Furthermore, S_1 and S_2 are dense in $\mathbf{Q}^+$, and thus in $\mathbf{R}^+$.

In fact, given $r \in \mathbf{Q}^+ \setminus S_1, \exists p, q \in \mathbf{Z}^+$ such that $r = \frac{2p-1}{2q}$. Thus

$$r_k = \frac{2p - 1 - \frac{2}{2k}}{2q - \frac{1}{2k}} = \frac{(4kp - 2k - 2)/2k}{(4kq - 1)/2k} = \frac{2(2kp - 2k - 1)}{2(2kq) - 1} \in S_1 \quad \forall k = 1, 2, 3, \ldots$$

and $\lim_{k \to \infty} r_k = (2p - 1)/2q = r$. That is, $\overline{S}_1 \supseteq \mathbf{Q}^+$. Similarly, $\overline{S}_2 \supseteq \mathbf{Q}^+$.

PROPOSITION 5.3. *For characteristic equation*

$$\lambda^k + \sum_{j=1}^{k-1} a_j \lambda^j + b + ce^{-\lambda\sigma_1} + de^{-\lambda\sigma_2} = 0, \quad k \ge 2,\ \sigma_1, \sigma_2 > 0, \tag{5.4}$$

where $b, c, d > 0, a_j \in \mathbf{R}, j = 1, 2, 3, \ldots, k$*, if* $b < d - c$ *or* $b < c - d$*, then* $\exists \sigma_{10} > 0$ *and* $\sigma_{20} > 0$ *such that the characteristic equation* (5.4) *has at least one root with positive real part for* $\sigma_1 > \sigma_{10}$ *and* $\sigma_2 > \sigma_{20}$ *provided* $\sigma_1/\sigma_2 \in S_1$ *or* $\sigma_1/\sigma_2 \in S_2$*.*

We need the following lemma to prove Proposition 5.3.

LEMMA 5.4. *For the equation*

$$\epsilon^k z^k + \sum_{j=1}^{k-1} a_j \epsilon^j z^j + b + ce^{-p_1 z} + de^{-p_2 z} = 0, \quad k \ge 2,\ p_1, p_2 > 0,\ z \in \mathbf{C}, \tag{5.5}$$

where $b, c, d > 0, a_j \in \mathbf{R}, j = 1, 2, 3, \ldots, k - 1$*, assume*

(i) $b < d - c$ *and* $p_1/p_2 \in S_1$, *or*
(ii) $b < c - d$ *and* $p_1/p_2 \in S_2$.

Then, $\exists \epsilon_0 > 0$ *such that for all* $\epsilon, 0 < \epsilon < \epsilon_0$, *equation* (5.5) *has at least one root with positive real part.*

The proof of Lemma 5.4 is given in Appendix C. Now we prove Proposition 5.3.

Proof. Assume $b < d - c$ and $\sigma_1/\sigma_2 \in S_1$ (or $b < c - d$ and $\sigma_1/\sigma_2 \in S_2$). In Lemma 5.4, choose p_{10} and p_{20} such that $p_{10}/p_{20} \in S_1$ (or $p_{10}/p_{20} \in S_2$). Suppose ϵ_0 is given by inequality (C.2) in the proof of Lemma 5.4. Let $\sigma_{10} = p_{10}/\epsilon_0$ and $\sigma_{20} = p_{20}/\epsilon_0$. Then given $\sigma_1 > \sigma_{10}$, $\sigma_2 > \sigma_{20}$, and $\sigma_1/\sigma_2 \in S_1$ (or $\sigma_1/\sigma_2 \in S_2$), $\exists \epsilon$, $0 < \epsilon < \epsilon_0$, such that

$$\sigma_1 = p_1/\epsilon > \sigma_{10} \quad \text{and} \quad \sigma_2 = p_2/\epsilon > \sigma_{20}.$$

Let $\lambda = \epsilon z$. Then (5.4) becomes (5.5) in Lemma 5.4 and the conclusion follows. ∎

Remark. In Lemma 5.4, given p_1 and p_2, $p_1/p_2 \in S_1$ in case (i) or $p_1/p_2 \in S_2$ in case (ii), if we carefully choose ϵ_0 in the proof of Lemma 5.4, an estimate of unstable region of σ_1 and σ_2 can be given. For the special case $k = 2$, r_0 and ϵ_0 can be chosen as

$$r_0 = \sqrt{K^2 x_0^2 + q^2 \pi^2} \quad \text{and} \quad \epsilon_0 = \left(\sqrt{a_1^2 + 4\eta_0'} - a_1 \right) / 2r_0.$$

Let $k = 2$ and apply Proposition 5.3 to the linearized system (4.1). We have the following.

PROPOSITION 5.5. *If* $d_i A < D|C - B|$, *then there exist* $\tau_{10} > 0$ *and* $\tau_{20} > 0$ *such that the characteristic equation of system* (4.1) *has at least one root with positive real part if*

(i) $d_i A < D(C - B)$, $\tau_1 > \tau_{10}$, $\tau_1 + \tau_2 > \tau_{20}$, *and* $\tau_1/(\tau_1 + \tau_2) \in S_1$, *or*
(ii) $d_i A < D(B - C)$, $\tau_1 > \tau_{10}$, $\tau_1 + \tau_2 > \tau_{20}$, *and* $\tau_1/(\tau_1 + \tau_2) \in S_2$.

Proof. This is straightforward if in Proposition 5.3 we choose $k = 2, a_1 = A + d_i, b = d_i A, c = DB, d = DC, \sigma_1 = \tau_1$, and $\sigma_2 = \tau_1 + \tau_2$. ∎

Therefore, we have the following theorem.

THEOREM 5.6. *In model* (2.1), *let*

$$H_2(d_i, G_{in}) := D|C - B| - d_i A. \tag{5.6}$$

If $\tau_1 > 0$, $\tau_2 > 0$, *and* $H_2(d_i, G_{in}) > 0$, *then there exist* $\tau_{10} > 0$ *and* $\tau_{20} > 0$ *such that the steady state* (G^*, I^*) *is unstable when* $\tau_1 > \tau_{10}$, $\tau_1 + \tau_2 > \tau_{20}$ *and*

(i) $\tau_1/(\tau_1 + \tau_2) \in S_1$ *and* $d_i A < D(C - B)$, *or*
(ii) $\tau_1/(\tau_1 + \tau_2) \in S_2$ *and* $d_i A < D(B - C)$.

Remark. Using the function (6.1)–(6.5), if $G_{in} = 1.35$ and $d_i = 0.06$, then $H_2(d_i, G_{in}) > 0$ and $H_1(d_i, G_{in}) < 0$. According to Theorem 5.6, the steady state will lose its stability as the delays increase. Let $\tau_1 = 7$ and $\tau_2 = 30$. The simulation result is shown in Figure 5.1 (left). There exists a periodic solution bifurcating from the steady state. This periodic solution can be regarded as the sustained oscillation of the insulin and glucose concentration. The period of the periodic solution is approximately 149 minutes. In each cycle, the glucose concentration peaks about 18 minutes ahead of the insulin concentration peaks. The varying range of glucose concentration is within physiological meaningful scope [70, 109].

Remark. It is clear that $H_2(d_i, G_{in}) \leq H_1(d_i, G_{in})$. When $H_1(d_i, G_{in}) \leq 0$, the steady state of model (2.1) is stable due to Theorem 5.2. On the other hand, when $H_2(d_i, G_{in}) > 0$, according to Theorem 5.6, the steady state is unstable for appropriate delay values given in Theorem 5.6. With specific function (6.1)–(6.5), Figure 5.1

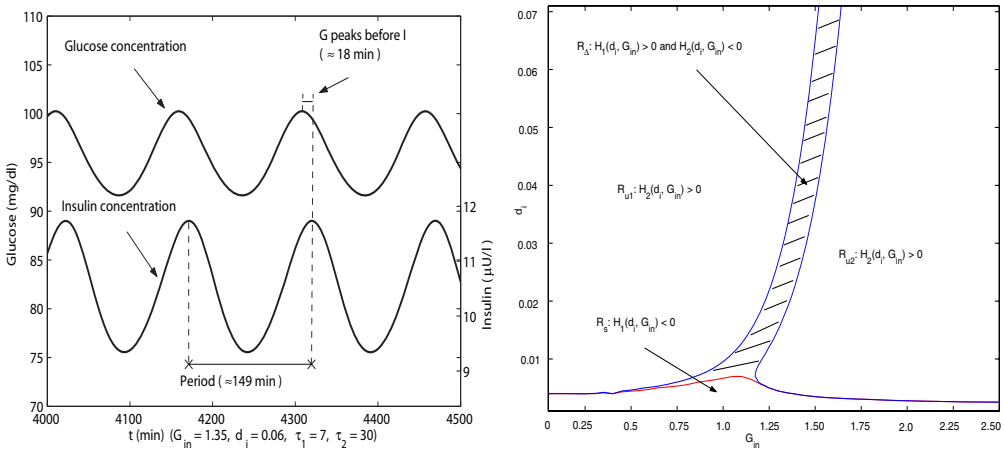

FIG. 5.1. *Left: The periodic solution of model* (2.1) *when* $G_{in} = 1.35, d_i = 0.06, \tau_1 = 7$, *and* $\tau_2 = 30$. *The period is approximately* 149 *minutes and the glucose concentration peaks about* 18 *minutes before the insulin concentration peaks. Right: Regions in the* (G_{in}, d_i)*-plane divided by curves* $H_1(d_i, G_{in}) = 0$ *and* $H_2(d_i, G_{in}) = 0$. *When* $d_i \in R_s$, *the steady state of model* (2.1) *is stable; when* $d_i \in R_{u1} \cup R_{u2}$, *the steady state is unstable.*

(right) shows the delay-independent stable region R_s and delay-dependent unstable region R_{u1} and R_{u2} in the (d_i, G_{in})-plane determined by Theorems 5.2 and 5.6, respectively. The shaded region R_Δ is where $H_1(d_i, G_{in}) > 0$ and $H_2(d_i, G_{in}) \le 0$. The local stability problem of (G^*, I^*) is open when $(d_i, G_{in}) \in R_\Delta$. Our intensive numerical simulations reveal that R_Δ is also a delay-dependent unstable region, that is, with appropriate delay parameters, the steady state is unstable. For example, when $d_i = 0.051$ and $G_{in} = 1.50$, $H_1(0.051, 1.50) = 0.0019$ and $H_2(0.051, 1.50) = -0.00042570$. The steady state is unstable when $\tau_1 \ge 15$ and $\tau_2 \ge 32$. When $d_i = 0.0320$ and $G_{in} = 1.40$, $H_1(0.0320, 1.40) = 0.00099732$ and $H_2(0.051, 1.50) = -0.00026753$. The steady state is unstable when $\tau_1 \ge 18$ and $\tau_2 \ge 36$. Periodic solutions are also observed in these cases.

5.3. Hopf bifurcation. We show below that a local Hopf bifurcation takes place when delay parameter τ_1 or τ_2 varies. It has been shown that when $\tau_1 = 0$ ($\tau_2 = 0$), the steady state of system (2.1) is stable provided that τ_2 (τ_1) is small enough (see Theorem 4.2). To show this system undergoes a unique local Hopf bifurcation at some $\bar\tau_1 > 0$ ($\bar\tau_2 > 0$) as τ_1 (τ_2) increases from 0 and within a physiologically meaningful range, we prove that the characteristic equation (4.3) has a pair of pure conjugate imaginary simple roots at $\tau_1 = \bar\tau_1 > 0$ ($\tau_2 = \bar\tau_2 > 0$) and all such roots cross the imaginary axis from left to right. This indicates that a periodic solution is generated from this stability switch. Our numerical simulations show that the bifurcation is indeed supercritical.

Consider equation

$$\omega^4 + (A^2 + d_i^2)\omega^2 + d_i^2 A^2 = D^2(B^2 + C^2 + 2BC). \tag{5.7}$$

Clearly, (5.7) has a unique positive root $\hat\omega$ when $d_i A < D(B + C)$, where

$$\hat\omega^2 = \frac{1}{2}\Big[-(A^2 + d_i^2) + \sqrt{(A^2 + d_i^2) - 4(d_i^2 A^2 - D^2(B + C)^2)}\Big]. \tag{5.8}$$

Let $g(\omega) = \omega^4 + (A^2 + d_i^2)\omega^2 + d_i^2 A^2 - D^2(B^2 + C^2 + 2BC\cos\omega\tau_2)$. Then (5.2) can be written as $g(\omega) = 0$. If $\omega < \hat{\omega} < \frac{\pi}{2\tau_2}$, then $g(0) = d_i^2 A^2 - D^2(B + C)^2 < 0$ and $g(\hat{\omega}) = 2D^2BC(1 - \cos\omega\tau_2) \geq 0$. Further, $g'(\omega) = 4\omega^3 + 2(A^2 + d_i^2)\omega + 2D^2BC\sin\omega\tau_2 > 0$ for $0 < \omega < \hat{\omega} \leq \frac{\pi}{2\tau_2}$. Therefore we have the following lemma.

LEMMA 5.7. *If $d_iA < D(B + C)$ and $\tau_2 < \frac{\pi}{2\hat{\omega}}$, then (5.2) has a unique root ω_0 with $0 < \omega_0 \leq \hat{\omega}$.*

The following propositions establish sufficient conditions for the existence of Hopf bifurcation when τ_1 or τ_2 varies. We leave the proofs in Appendices D and E.

PROPOSITION 5.8. *If $H_1(G_{in}, d_i) = D(B + C) - d_iA > 0$ and $\tau_1 + \tau_2 < \frac{\pi}{2\hat{\omega}}$, then (4.1) undergoes a Hopf bifurcation when τ_1 increases from 0 to $\frac{\pi}{2\hat{\omega}} - \tau_2$ for given τ_2.*

PROPOSITION 5.9. *If $H_1(G_{in}, d_i) = D(B + C) - d_iA > 0, \tau_1 + \tau_2 < \frac{\pi}{2\hat{\omega}}$, and $\tau_1 < \frac{A+d_i}{DB}$, then (4.1) undergoes a Hopf bifurcation when τ_2 increases from 0 to $\frac{\pi}{2\hat{\omega}} - \tau_1$ for given τ_1.*

Remark. Using the specific functions (6.1)–(6.5) given in section 6, for $(G_{in}, d_i) \in [0, 150] \times [0.001, 0.07]$, approximately, $47.2665 < \frac{\pi}{2\hat{\omega}} < 214.3462$ and $19.6857 < \frac{A+d_i}{DB} < 6361.7$. Thus τ_1 varies within its physiological range under the condition $\tau_1 < \frac{A+d_i}{DB}$. Under the condition $\tau_1 + \tau_2 < \frac{\pi}{2\hat{\omega}}$, both τ_1 and τ_2 are within their physiological meaningful ranges in most situations for $(G_{in}, d_i) \in [0, 150] \times [0.001, 0.07]$. When $\tau_1 + \tau_2$ could be larger than 47.2665, our simulations show that the Hopf bifurcation does exist and it is supercritical.

We summarize the above results in the following theorem.

THEOREM 5.10. *For model (2.1), assume $H_1(G_{in}, d_i) = D(B + C) - d_iA > 0$ and $\tau_1 + \tau_2 < \frac{\pi}{2\hat{\omega}}$.*

(a) *Then there exists a $\bar{\tau}_1 > 0$ such that the steady state (G^*, I^*) is stable when $\tau_1 < \bar{\tau}_1$, and unstable when $\tau_1 \geq \bar{\tau}_1$. The system undergoes a Hopf bifurcation at $\bar{\tau}_1$ and generates a periodic solution.*

(b) *Further, assume $\tau_1 < \frac{A+d_i}{DB}$. Then there exists a $\bar{\tau}_2 > 0$ such that the steady state (G^*, I^*) is stable when $\tau_2 < \bar{\tau}_2$, and unstable when $\tau_2 \geq \bar{\tau}_2$. The system undergoes a Hopf bifurcation at $\bar{\tau}_2$ and generates a periodic solution.*

Remark. With the specific functions (6.1)–(6.5) in the next section, our intensive numerical simulations show that the Hopf bifurcations determined by Theorem 5.10 are supercritical. Moreover, with $G_{in} = 1.35$ and $d_i = 0.06$, $\bar{\tau}_1$ and $\bar{\tau}_2$ approximately satisfy $33.9\bar{\tau}_1 + 17.3\bar{\tau}_2 \approx 36.9$ for $0 \leq \bar{\tau}_1 \leq 20$ and $0 \leq \bar{\tau}_2 \leq 60$.

6. Numerical simulations. In this section, we present numerical analysis on model (2.1) using DDE23 [22] in MATLAB 6.5. We use the same functions $f_i, i = 1, 2, 3, 4, 5$, as [2], [17], [25], and [26] given in (6.1)–(6.5). The parameters, listed in Table 6.1, were generated from experiments [25], [26].

$$f_1(G) = R_m/(1 + \exp((C_1 - G/V_g)/a_1)), \tag{6.1}$$

$$f_2(G) = U_b(1 - \exp(-G/(C_2V_g))), \tag{6.2}$$

$$f_3(G) = G/(C_3V_g), \tag{6.3}$$

$$f_4(I) = U_0 + (U_m - U_0)/(1 + \exp(-\beta\ln(I/C_4(1/V_i + 1/Et_i)))), \tag{6.4}$$

$$f_5(I) = R_g/(1 + \exp(\alpha(I/V_p - C_5))). \tag{6.5}$$

TABLE 6.1
Parameters of the functions in two-time-delay model (2.1).

Parameters	Units	Values	Parameters	Units	Values
V_g	l	10	R_m	$\mu U \min^{-1}$	210
a_1	$\text{mg} \cdot \text{l}^{-1}$	300	C_1	$\text{mg} \cdot \text{l}^{-1}$	2000
U_b	$\text{mg} \cdot \min^{-1}$	72	C_2	$\text{mg} \cdot \text{l}^{-1}$	144
C_3	$\text{mg} \cdot \text{l}^{-1}$	1000	U_0	$\text{mg} \cdot \min^{-1}$	40
U_m	$\text{mg} \cdot \min^{-1}$	940	β		1.77
C_4	μUl^{-1}	80	R_g	$\text{mg} \cdot \min^{-1}$	180
α	$\text{l}\mu\text{U}^{-1}$	0.29	C_5	μUl^{-1}	26

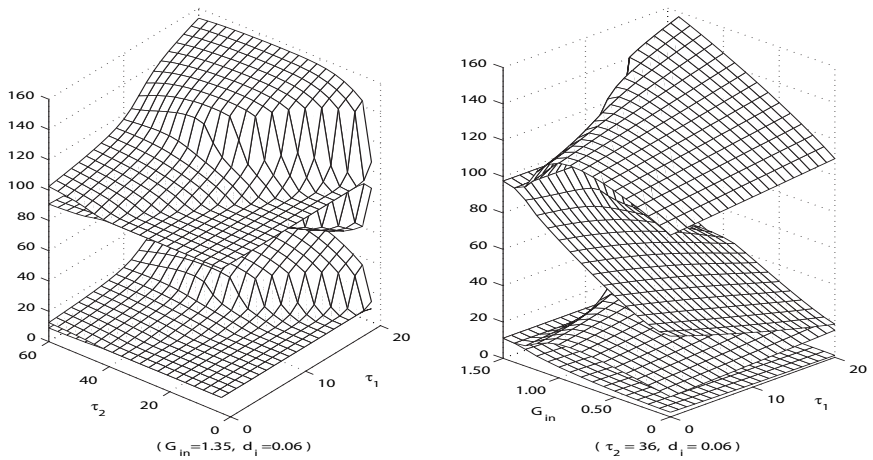

FIG. 6.1. *Limiting values or amplitudes of glucose (top) and insulin (bottom) concentrations when τ_1 and τ_2 vary (left) or G_{in} and τ_1 vary (right).*

The simulations in [17] focused on the bifurcation when a single parameter varies while other parameters are fixed. The detected bifurcation points of the varying parameters can determine when the sustained oscillations occur. In this section, we carry out a sequence of two-parameter bifurcation analyses and depict their quantitative behaviors in three-dimensional meshes or two-dimensional curves formed by transversal points.

For a specific subject, the insulin response time delay, the delayed effect of hepatic glucose production, and the insulin degradation rate are intrinsic. But the exogenous glucose infusion rate is controllable by diet, fasting, and so on. So, in addition to the simulation on the two-delay parameters, we numerically analyze the relationships of the glucose infusion rate G_{in} vs. the insulin response time delay τ_1, the hepatic glucose production time delay τ_2, and the insulin degradation rate d_i, respectively. We end this section by showing the significant impact of the two delays on generating insulin ultradian oscillation.

6.1. Insulin response delay τ_1 vs. hepatic glucose production delay τ_2. We analyzed the relationship between the insulin response delay τ_1 and the hepatic glucose production delay τ_2 while $G_{in} = 1.35$ and $d_i = 0.06$ are fixed. Figure 6.1 (left) shows that a simple curve ($33.9\tau_1 + 17.3\tau_2 \approx 36.9$ for $0 \le \tau_1 \le 20$ and $0 \le \tau_2 \le 60$)

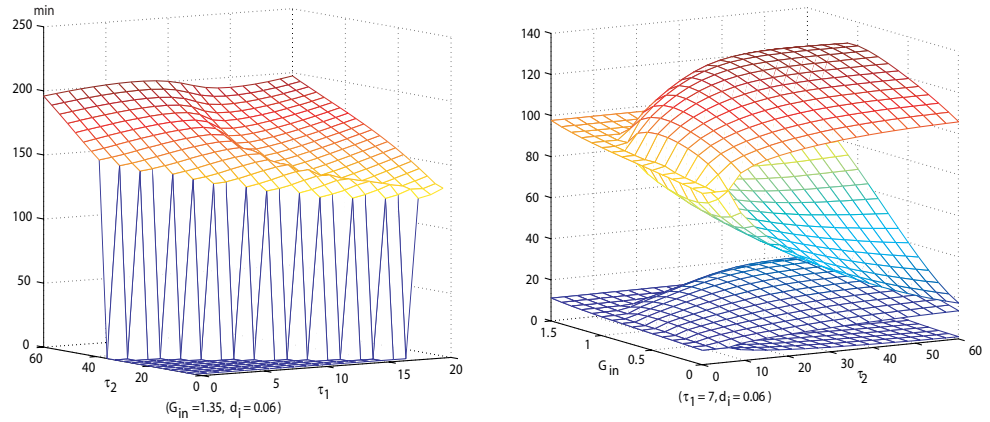

FIG. 6.2. *Left: Mesh of the periods of periodic solutions when* $(\tau_1, \tau_2) \in [0, 20] \times [0, 60]$*, where* $G_{in} = 1.35$ *and* $d_i = 0.06$ *are fixed. Right: Meshes of the amplitudes of glucose and insulin concentrations when* $(G_{in}, \tau_2) \in [0, 1.5] \times [0, 60]$*, where* $\tau_1 = 7$ *and* $d_i = 0.06$ *are fixed.*

divides $[0, 20] \times [0, 60]$ in the (τ_1, τ_2)-plane into two regions. The steady state is stable in one region and unstable in the other. The sustained oscillations occur in the unstable region which requires both $\tau_1 > 0$ and $\tau_2 > 0$ to be sufficiently large. The top and bottom meshes in Figure 6.1 (left) demonstrate the amplitudes of glucose and insulin concentrations, respectively. The periods of periodic solutions are shown in Figure 6.2 (left). According to Figure 6.1 (left) and Figure 6.2 (left), the amplitudes of glucose concentration are between 70 and 109 and the periods of periodic solutions are approximately within 90 and 150 when $\tau_1 \in (5, 15)$ and $\tau_2 \in (25, 50)$. There is a sudden jump of amplitudes of glucose and insulin concentrations when $\tau_1 > 10$ approximately. Also, in such cases, the periods of periodic solutions decrease.

6.2. Glucose infusion rate G_{in} vs. insulin response time delay τ_1. Taking both insulin response delay τ_1 and glucose infusion rate G_{in} as bifurcation parameters, we try to identify the stability regions when $(\tau_1, G_{in}) \in [0, 20] \times [0, 1.5]$. Let $d_i = 0.06$ and $\tau_2 = 36$ be fixed. The computation results are shown in Figure 6.1 (right). The bifurcation point value $\bar{\tau}_1 \approx 1.0429 G_{in} - 1.3740 > 0$ exists for $1.3175 \leq G_{in} \leq 1.50$. The meshes are the amplitudes of glucose (top) and insulin (bottom) concentrations when $(\tau_1, G_{in}) \in [0, 20] \times [0, 1.5]$. It can be seen that a simple curve ($\tau_1 \approx 1.0429 G_{in} - 1.3740 > 0$ for $1.3175 \leq G_{in} \leq 1.50$) divides the rectangular $[0, 20] \times [0, 1.5]$ in the (τ_1, G_{in})-plane into two regions. The sustained oscillations of model (2.1) occur in the unstable region. The exogenous glucose infusion rate can be larger when τ_1 increases from [5, 15] for sustained regulatory oscillations to occur.

6.3. Glucose infusion rate G_{in} vs. hepatic glucose production delay τ_2. As shown in Figure 6.2 (right), our simulation results indicate that when $\tau_1 = 7$ and $d_i = 0.06$, the rectangular $[0, 60] \times [0, 1.50]$ in the (τ_2, G_{in})-plane is divided by a simple curve into two regions. The steady state of model (2.1) is unstable in the unstable region and the oscillations are sustained. The periods of periodic solutions are in a range of 80 and 195 minutes (not shown). The simple curve is determined by the Hopf bifurcation point values $\bar{\tau}_2(G_{in})$ as G_{in} varies from 0 to 150. The relationship between G_{in} and $\bar{\tau}_2$ is nonlinear. For example, $\bar{\tau}_2 \approx 6.1, 2.8, 6.1, 9, 12, 18, 33$ when

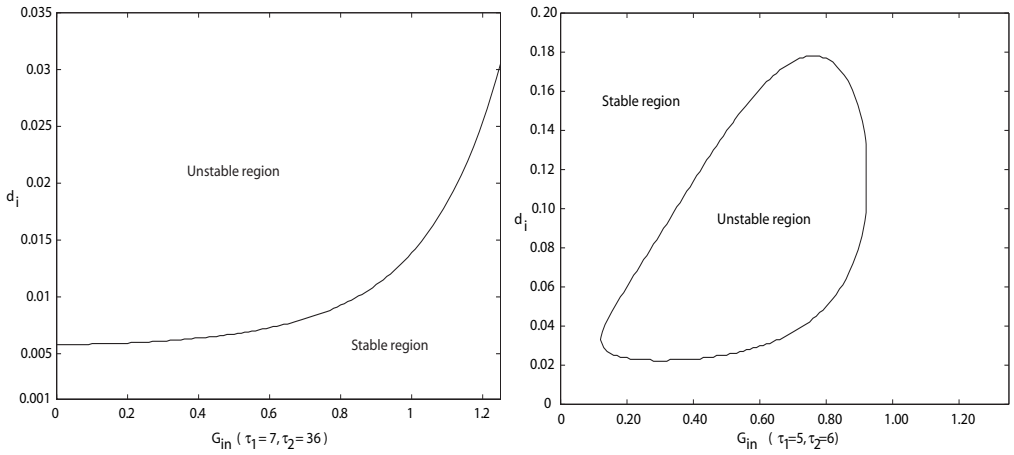

FIG. 6.3. *Left: Insulin degradation rate d_i vs. glucose infusion rate G_{in} while $\tau_1 = 7$ and $\tau_2 = 36$. The steady state of model (2.1) is stable in one region and unstable in the other. Right: Stable and unstable regions of the steady state when $\tau_1 = 5$ and $\tau_2 = 6$.*

$G_{in} = 0, 0.60, 0.80, 1.10, 1.20, 1.30, 1.40$, respectively. Similar to the case of G_{in} vs. τ_1, the exogenous glucose infusion rate can be larger when τ_2 increases from 10 to 60 minutes for sustained regulatory oscillations to occur. When $\tau_2 < 2$, the steady state is stable and no sustained oscillation will occur regardless of what value G_{in} assumes.

6.4. Glucose infusion rate G_{in} vs. insulin degradation rate d_i. Similarly, taking both glucose infusion rate G_{in} and insulin degradation rate d_i as bifurcation parameters while $\tau_1 = 7$ and $\tau_2 = 36$ are fixed, we identified the stability regions in $(G_{in}, d_i) \in [0, 1.35] \times [0.001, 0.20]$. Figure 6.3 shows that a simple curve divides the rectangular $(G_{in}, d_i) \in [0, 1.35] \times [0.001, 0.20]$ into two regions (the figure shows the part of $[0, 1.35] \times [0.001, 0.035]$ only). The steady state of model (2.1) is stable in one region and unstable in the other region. It is clear that larger insulin degradation rate d_i facilitates the oscillatory regulation. However, if $d_i = 1.75$ is large, then no self-sustained oscillation occurs. This suggests that d_i needs to be in moderate range for oscillations to be sustained. Let $\tau_1 = 5$ and $\tau_2 = 6$ be smaller. Figure 6.3 (right) shows that the sustained oscillation occurs in a region surrounded by a closed curve, which requires both d_i and G_{in} to be in moderate ranges. Our simulation shows that the amplitudes of the sustained oscillations are very small ($G \in (80, 100)$ and $I \in (10, 12)$) with periods from 58 to 105 minutes. This shows that when the delays τ_1 and τ_2 are smaller, both the insulin clearance rate and the glucose infusion rate have to be in a moderate range to ensure the oscillatory behavior of insulin secretion.

7. Discussions. In this paper, we studied the glucose-insulin regulatory system model (2.1) analytically and numerically. Compared with the observations obtained in [2], [17], [25], and [26], our work confirms most of the known observations and yields additional insightful information. Using the notation in [17], we refer to the observations in [25] and [26] as [STx] ([ST1]–[ST4]), the observations in [2] as [BGx] ([BG1] and [BG2]), and the observations in [17] as [Ax] ([A1]–[A9]). We conclude this paper with a list of remarks and new observations (denoted by [Bx]).

[B1] Theorem 4.2 reveals that the delays in the glucose-insulin regulatory system are critical for ensuring the sustained oscillations of regulation and

insulin secretions. Particularly, the role of delay of insulin secretion and the newly synthesized insulin becoming remote insulin is more critical than the role of delay of hepatic glucose production.

[B2] If the insulin secretion responds to elevated glucose instantaneously, that is, $\tau_1 = 0$, Theorem 4.2 (c.1) and (c.2) reveal that the insulin degradation rate for sustaining oscillation is likely to be lower than that in the case of $\tau_1 > 0$ and $\tau_2 = 0$ (Theorem 4.2 (b.1) and (b.2)). This suggests that the oscillatory behavior of the glucose-insulin regulation requires the insulin removal rate to be large enough ($H_2(d_i, G_{in}) > 0$) and the delayed effect of hepatic glucose production to be long enough ($\tau_2 > \tau_{20}$).

[B1] and [B2] analytically confirm the numerical observation of [ST3]. It demonstrates that the effort of dividing insulin into two compartments in the model can be and shall be naturally and explicitly replaced by the delay parameter τ_1.

[B3] According to Theorem 4.2 (b.1) for $\tau_1 = 0$, and Theorem 5.2 for $\tau_2 > 0$, the insulin degradation rate d_i has to be "large" enough for sustained oscillatory regulation of the glucose-insulin metabolic system. Here the meaning of "large" refers to the numerical simulation demonstrated in Figure 5.1 (right) that $H_1(d_i, G_{in}) > 0$. This confirms the observation [BG1] in [2].

[B4] When $\tau_1\tau_2 > 0$, Theorem 5.6, Theorem 5.10, and simulations in Figure 5.1 (right) reveal the intrinsic relationship among d_i, G_{in}, τ_1, and τ_2 to secure the oscillatory behavior of the metabolic system. That is, for a subject, the oscillatory regulation occurs if one's insulin degradation rate and the glucose infusion rate satisfy $H_2(d_i, G_{in}) > 0$, and the time delays in the system are long enough ($\tau_1 > \tau_{10}$ and $\tau_1 + \tau_2 > \tau_{20}$). The numerical observations in Figure 6.3 (left) indicate that if the insulin degradation rate is sufficiently small ($H_1(d_i, G_{in}) < 0$), the oscillations cannot be sustained. Small d_i causes the insulin concentration level to remain high in plasma, which prohibits the glucose concentration level to rise. In such cases, the oscillatory regulation does not occur. This provides more insightful information than the general statements in [BG1] and [A7]. On the other hand, Figure 6.3 (right) indicates that both the glucose infusion rate and the insulin clearance rate are sensitive to the delays τ_1 and τ_2. Both rates are required to be in moderate ranges for sustained oscillations when the delayed effects are shorter.

[B5] Figures 6.1 (right), 6.2 (right), and 6.3 (left) show that when the glucose infusion rate is high, the oscillation of insulin secretion is unlikely to persist. This is possibly due to the fact that the β-cells cannot produce and secrete enough insulin to uptake the large amount of glucose infused into plasma. Thus the glucose concentration remains at a high level. The result is that the ultradian oscillations of insulin secretion and the oscillatory regulation of the glucose-insulin metabolic system cannot be sustained. This may help to explain the observed steady state behavior in models of the intravenous glucose tolerance test (IVGTT) where initial glucose infusion values are high [3], [9], [16], [19].

[B6] In the IVGTT, the initial glucose infusion is large. Compared to such large exogenous glucose infusion, the hepatic glucose production is negligible. For this reason, IVGTT models are justified not to include the hepatic glucose production term explicitly (set $f_5 \equiv 0$ thus $\tau_2 = 0$) [3], [9], [16], and [19]. The main goal of these models is to accurately monitor the dynamical behavior of the glucose level, which must return to its basal level after the biphasic insulin secretions have been triggered. Thus the insulin sensitivity can be

tested. The simulations (Figures 1 and 2) in [16] reveal that the delay τ_1 has to be extremely large (> 400 minutes) to produce any sustainable oscillations. Such a huge delay τ_1 clearly falls out of the normal physiological range.

Since we normally eat three meals per day, it is more plausible to consider periodic exogenous glucose infusion. That is, the constant glucose infusion rate G_{in} in model (2.1) shall be replaced by a periodic function $G_{in}(t)$ with a positive period ω between 180 and 300 minutes. Our simulation results reveal that there exists a harmonic solution in such a system. For more details, interested readers can refer to [24].

Appendix A. Proof of Proposition 3.2. For the first part of (i), let

$$H(x) = G_{in} - f_2(x) - f_3(x)f_4(d_i^{-1}f_1(x)) + f_5(d_i^{-1}f_1(x)) = 0, \quad x \geq 0. \tag{A.1}$$

We shall show that (A.1) has a unique root in $[0, \infty)$. Observing that $f_1'(x) > 0$, $f_2'(x) > 0$, $f_4'(x) > 0$, $f_3'(x) > 0$, and $f_5'(x) < 0$, we have $H'(x) < 0$. Notice that $H(0) = G_{in} - f_2(0) - f_3(0)f_4(d_i^{-1}f_1(0)) + f_5(d_i^{-1}f_1(0)) = G_{in} + f_5(d_i^{-1}f_1(0)) > 0$, and

$$\begin{aligned}
\lim_{x\to\infty} H(x) &= G_{in} - \lim_{x\to\infty} f_2(x) - \lim_{x\to\infty} f_3(x)f_4(d_i^{-1} \lim_{x\to\infty} f_1(x)) + f_5(d_i^{-1} \lim_{x\to\infty} f_1(x)) \\
&= G_{in} - M_2 - f_4(d_i^{-1}M_1) \lim_{x\to\infty} f_3(x) + f_5(d_i^{-1}M_1) \\
&< G_{in} - M_2 - m_4 \lim_{x\to\infty} f_3(x) + M_5 < 0.
\end{aligned}$$

In addition, $f_1(x)$ is strictly monotone increasing, so the proof is complete. It is obvious that G^* is the root of (A.1) and $I^* = d_i^{-1}f_1(G^*)$.

For the second part of (i), observing that $|f_i'(x)|$, $i = 1, 2, 3, 4, 5$, are bounded, $f_i(x), i = 2, 3, 4$, and $f_j(x_t), j = 1, 5$, are *Lipschitzian* and completely continuous in $x \geq 0$ and $x_t \in \mathbf{C}([-\max\{\tau_1, \tau_2\}, 0])$, respectively. Then by Theorems 2.1, 2.2, and 2.4 on pp. 19 and 20 in [15], the solution of (2.1) with given initial condition exists and is unique for all $t \geq 0$. If there exists a $t_0 > 0$ such that $G(t_0) = 0$ and $G(t) > 0$ for $0 < t < t_0$, then $G'(t_0) \leq 0$. So

$$\begin{aligned}
0 \geq G'(t_0) &= G_{in} - f_2(G(t_0)) - f_3(G(t_0))f_4(I(t_0)) + f_5(I(t_0 - \tau_2)) \\
&= G_{in} - f_2(0) - f_3(0)f_4(I(t_0)) + f_5(I(t_0 - \tau_2)) \\
&= G_{in} + f_5(I(t - \tau_2)) > 0.
\end{aligned}$$

This contradiction implies that $G(t) > 0$ for all $t > 0$. If $\exists t_0' > 0$ such that $I(t_0') = 0$ and $I(t) > 0$ for all $0 < t < t_0'$, then $I(t_0^{'}) < 0$. Therefore, $0 > I(t_0') = f_1(G(t_0^{'}) - d_i I(t_0' - \tau_1) \geq f_1(G(t_0')) > 0$. This implies that $I(t) > 0$ for all $t > 0$.

Now we show that any given solution $(G(t), I(t))$ of model (2.1) is bounded for $t > 0$. In fact, if $\limsup_{t\to\infty} G(t) = \infty$, there exists a sequence $\{t_n\}_{n=1}^{\infty} \uparrow \infty$ such that $\lim_{n\to\infty} G(t_n) = \infty$ and $G'(t_n) \geq 0$. Thus $0 < G'(t_n) = G_{in} - f_2(G(t_n)) - f_3(G(t_n))f_4(I(t_n)) + f_5(I(t_n - \tau_2)) \leq G_{in} - f_2(G(t_n)) - f_3(G(t_n))m_4 + M_5$, and therefore

$$\begin{aligned}
0 \leq \lim_{n\to\infty} G'(t_n) &\leq G_{in} - \lim_{n\to\infty} f_2(G(t_n)) - m_4 \lim_{n\to\infty} f_3(G(t_n)) + M_5 \\
&\leq G_{in} - M_2 - m_4 \lim_{x\to\infty} f_3(x) + M_5 < 0.
\end{aligned}$$

This contradiction shows that there is an $M_G > 0$ such that $G(t) < M_G$ for all $t > 0$. From the second equation in (2.1), since $|f_1(x)| \leq M_1$, for all $\epsilon > 0$, $I'(t) \leq f_1(M_G +$

$\epsilon) - d_i I(t)$ for sufficiently large $t > 0$. Then we have $\limsup_{t\to\infty} I(t) \le d_i^{-1} f_1(M_G+\epsilon)$. Since $\epsilon > 0$ is arbitrary, $\limsup_{t\to\infty} I(t) \le d_i^{-1} f_1(M_G) := M_I$.

If (ii) is not true, assume $\limsup_{t\to\infty} G(t) = M_G < \infty$. Then $\exists\{t_n\}_{n=1}^{\infty} \uparrow \infty$ such that $G'(t_n) = 0, n = 1, 2, 3, \ldots$, and $\lim_{n\to\infty} G(t_n) = M_G$ according to Lemma 3.1. Thus $G'(t_n) = G_{in} - f_2(G(t_n)) - f_3(G(t_n))f_4(I(t_n)) + f_5(I(t_n - \tau_2)) \ge G_{in} - f_2(G(t_n)) - f_3(G(t_n))m_4$. Let $n \to \infty$; then $0 \ge G_{in} - f_2(M_G) - f_3(M_G)m_4$, that is, $f_3(M_G) \ge (G_{in} - f_2(M_G))/m_4$. On the other hand, $f_3(M_G) \le \lim_{x\to\infty} f_3(x) < (G_{in} - M_2)/m_4 \le (G_{in} - f_2(M_G))/m_4$.

Appendix B. Proof of Lemma 3.3. First we show that (3.2) holds. Due to Lemma 3.1 and part (i) of Proposition 3.2, there exists a sequence $\{t_k\}_{k=1}^{\infty} \uparrow \infty$, such that $I'(t_k) = 0, \lim_{k\to\infty} I(t_k) = \overline{I}$. Thus, $0 = I'(t_k) = f_1(G(t_k - \tau_1)) - d_i I(t_k)$ for all $k = 1, 2, 3, \ldots$. Therefore, $f_1(\overline{G}) - d_i I(t_k) \ge f_1(\overline{G}(t_k - \tau_1)) - d_i I(t_k)$ for $k = 1, 2, 3, \ldots$. Thus, $f_1(\overline{G}) - d_i \overline{I} \ge 0$. On the other hand, there exists a sequence $\{s_k\}_{k=1}^{\infty} \uparrow \infty$ such that $\lim_{k\to\infty} I(s_k) = \underline{I}$ and $I'(s_k) = 0$ for all $k > 0$. Hence, $f_1(\underline{G}) - d_i I(s_k) \le f_1(\underline{G}(s_k - \tau_1)) - d_i I(s_k)$ for $k = 1, 2, 3, \ldots$. Thus, $f_1(\underline{G}) - d_i \underline{I} \le 0$.

Now we show that (3.3) holds. Again, due to Proposition 3.2 and Lemma 3.1, there exists a sequence $\{t_k'\}_{k=1}^{\infty} \uparrow \infty$ as $k \to \infty$ such that $\lim_{k\to\infty} G(t_k') = \overline{G}$ and $0 = G'(t_k') = G_{in} - f_2(G(t_k')) - f_3(G(t_k'))f_4(I(t_k')) + f_5(I(t_k' - \tau_2))$, $k = 1, 2, 3, \ldots$. Notice that $f_5 \downarrow 0$ and f_4 is monotone increasing and bounded from above by M_4; thus $0 = G_{in} - f_2(G(t_k')) - f_3(G(t_k'))f_4(I(t_k')) + f_5(I(t_k' - \tau_2)) \le G_{in} - f_2(G(t_k')) - f_3(G(t_k'))f_4(\underline{I}) + f_5(\underline{I}), k = 1, 2, 3, \ldots$, and thus $G_{in} - f_2(\overline{G}) - f_3(\overline{G})f_4(\underline{I}) + f_5(\underline{I}) \ge 0$.

Similarly we can show that (3.4) is true. According to part (i) of Proposition 3.2 and Lemma 3.1, there exists a sequence $\{s_k'\}_{k=1}^{\infty} \uparrow \infty$ as $k \to \infty$ such that $\lim_{k\to\infty} G(s_k') = \overline{G}$ and $0 = G'(s_k') = G_{in} - f_2(G(s_k')) - f_3(G(s_k'))f_4(I(s_k')) + f_5(I(s_k' - \tau_2)), k = 1, 2, 3, \ldots$. Notice that $f_5 \downarrow 0$ and f_4 is monotone increasing and bounded from above by M_4; thus $0 = G_{in} - f_2(G(s_k')) - f_3(G(s_k'))f_4(I(s_k')) + f_5(I(s_k' - \tau_2)) \ge G_{in} - f_2(G(s_k')) - f_3(G(s_k'))f_4(\overline{I}) + f_5(\overline{I}), k = 1, 2, 3, \ldots$. This leads to $G_{in} - f_2(\underline{G}) - f_3(\underline{G})f_4(\overline{I}) + f_5(\overline{I}) \le 0$.

Appendix C. Proof of Lemma 5.4. Let $f(z) = b + ce^{-p_1 z} + de^{-p_2 z}$. We show that $f(z)$ has a zero with positive real part. Since $p_1/p_2 \in S_1$ in case (i) ($p_1/p_2 \in S_2$ in case (ii)), there exist integers $m, n \ge 1$ such that $\frac{p_1}{p_2} = \frac{2m}{2n-1}$ for case (i), or $\frac{p_1}{p_2} = \frac{2m-1}{2n}$ for case (ii). Let $z = x + q\pi i$, where $q = 2m/p_1 = (2n-1)/p_2$ for case (i) or $q = (2m-1)/p_1 = 2n/p_2$ for case (ii). Then

$$\begin{aligned} f(z) &= b + ce^{-p_1 x}e^{-p_1 q\pi i} + de^{-p_2 x}e^{-p_2 q\pi i} \\ &= b + ce^{-p_1 x}\cos 2m\pi + de^{-p_2 x}\cos(2n-1)\pi \\ &\qquad (= b + ce^{-p_1 x}\cos(2m-1)\pi + de^{-p_2 x}\cos 2n\pi \text{ for case (ii)}) \\ &= b + ce^{-p_1 x} - de^{-p_2 x} \qquad (= b - ce^{-p_1 x} + de^{-p_2 x} \text{ for case (ii)}) \\ &:= H(x). \end{aligned}$$

Notice that $H(0) = b + c - d < 0$ ($H(0) = b - c + d < 0$ for case (ii)) and $\lim_{x\to\infty} H(x) = b > 0$; therefore $H(x)$ has at least one zero $x_0 \in (0, \infty)$. So $f(z)$ has at least one zero $z_0 = x_0 + q\pi i$ with $x_0 > 0$.

We perturb $f(z)$ by $g_\epsilon(z)$ given by

$$g_\epsilon(z) = \epsilon^k z^k + \sum_{j=1}^{k-1} a_j \epsilon^j z^j, \quad \epsilon > 0, \tag{C.1}$$

with small $\epsilon > 0$ and show that $f(z) + g_\epsilon(z)$ has the same number of zeros as $f(z)$ if ϵ is small. To this end, we first construct a simple loop γ homotopic to a point and then show $|f(z)| > |g_\epsilon(z)|$ on γ. Let $z = x$, $x \in (-\infty, \infty)$; then $|f(z)| = b + ce^{-p_1 x} + de^{-p_2 x} > b$. Let $z = x + 2q\pi i$, $x \in (-\infty, \infty)$; then

$$\begin{aligned}|f(z)| &= |b + ce^{-p_1 x} e^{2qp_1\pi i} + de^{-p_2 x} e^{2qp_2\pi i}| \\ &= |b + ce^{-p_1 x} \cos 4m\pi + de^{-p_2 x} \cos 2(2n-1)\pi| \\ &\qquad (= |b + ce^{-p_1 x} \cos 2(2m-1)\pi + de^{-p_2 x} \cos 4n\pi| \text{ for case (ii)}) \\ &= b + ce^{-p_1 x} + de^{-p_2 x} > b.\end{aligned}$$

Let $z = Kx_0 + yi$, $y \in [0, 2q\pi]$, where $K > 1$ such that $b - ce^{-p_1 K x_0} - de^{-p_2 K x_0} > b/2$. Then

$$\begin{aligned}|f(z)| &= |b + ce^{-p_1 K x_0} e^{-p_1 yi} + de^{-p_2 K x_0} e^{-p_2 yi}| \\ &\geq b - ce^{-p_1 K x_0} - de^{-p_2 K x_0} > b/2.\end{aligned}$$

Let $z = yi$, $y \in [0, 2q\pi]$; then

$$\begin{aligned}|f(z)| &= |b + ce^{-p_1 yi} + de^{-p_2 yi}| \geq \begin{cases} d - c - b & \text{for case (i)}, \\ c - d - b & \text{for case (ii)} \end{cases} \\ &:= \eta_0 > 0.\end{aligned}$$

Let $\eta_0' := \min\{\eta_0, b/2\}$. Denote

$$\begin{aligned}\gamma := \{z = x + yi \in \mathbf{C} : z = x \text{ or } z = x \pm 2q\pi i, \quad x \in [0, Kx_0], \\ \text{or } z = yi \text{ or } z = Kx_0 + yi, \quad y \in [0, 2q\pi].\end{aligned}$$

$$\gamma^\circ := \{z = x + yi \in \mathbf{C} : 0 < x < Kx_0, \ -2q\pi < y < 2q\pi\}.$$

Clearly, γ is a simple loop homotopic to the original, $z_0 = x_0 + q\pi i \in \gamma^\circ$ and $|f(z)| > \eta_0'$ on γ. Choose $r_0 > 0$ such that $\gamma \subset \mathcal{A} := \{z \in \mathbf{C} : |z| < r_0\}$. Denote $\partial\mathcal{A} := \{z \in \mathbf{C} : |z| = r_0\}$. Thus for all $z \in \partial\mathcal{A}$, $z = r_0 e^{\theta i}$, $\theta \in [0, 2\pi]$, we have

$$|g_\epsilon(z)| = |\epsilon^k z^k + \sum_{j=1}^{k-1} a_j \epsilon^j z^j| \leq \epsilon^k r_0^k + \sum_{j=1}^{k-1} |a_j| \epsilon^j r_0^j. \tag{C.2}$$

Obviously $\exists \epsilon_0 > 0$ such that for all $\epsilon, 0 < \epsilon < \epsilon_0$, $|g_\epsilon(z)| < \eta_0', z \in \partial\mathcal{A}$. For all $z \in \mathcal{A}, z = re^{\theta i}$; then $r < r_0$, and

$$|g_\epsilon(z)| = |\epsilon^k z^k + \sum_{j=1}^{k-1} a_j \epsilon^j z^j| \leq \epsilon^k r^k + \sum_{j=1}^{k-1} |a_j| \epsilon^j r^j < \epsilon^k r_0^k + \sum_{j=1}^{k-1} |a_j| \epsilon^j r_0^j.$$

Thus $|g_\epsilon(z)| < \eta_0'$ for all $z \in \gamma$. Therefore $|f(z)| > |g_\epsilon(z)|$ on γ. By Rouchè's theorem [7, pp. 125–126], $f(z)$ and $f(z) + g_\epsilon(z)$ have the same number of zeros in γ°. That is, $f(z) + g_\epsilon(z) = 0$ has at least one root $\hat{z}_\epsilon \in \gamma^\circ$.

Appendix D. Proof of Proposition 5.8. We need only show that the conjugate roots of (4.3) cross the imaginary axis from left to right. Assume $\tau_1 + \tau_2 < \frac{\pi}{2\hat{\omega}}$. From (4.3), we have

$$\begin{aligned}&\Big[2\lambda + (A + d_i) - DBe^{-\lambda\tau_1}\tau_1 - DCe^{-\lambda(\tau_1+\tau_2)}(\tau_1 + \tau_2)\Big]\frac{d\lambda}{d\tau_1} \\ &= \Big(DBe^{-\lambda\tau_1} + DCe^{-\lambda(\tau_1+\tau_2)}\Big)\lambda.\end{aligned}$$

If the root $\lambda(\bar{\tau}_1) = i\omega$ is not simple for some $\bar{\tau}_1 > 0$, then $\frac{d\lambda}{d\tau_1}\big|_{\tau_1=\bar{\tau}_1} = 0$. Thus,

$$-DBe^{-i\omega\bar{\tau}_1} - DCe^{-i\omega\bar{\tau}_1+\tau_2}i\omega = 0 \quad \text{and} \quad (B + C\cos\omega\tau_2) - i\sin\omega\tau_2 = 0.$$

This is impossible since $\tau_2 < \frac{\pi}{2\hat{\omega}}$. Therefore,

$$\Big(\frac{d\lambda}{d\tau_1}\Big)^{-1} = \frac{[2\lambda + (A + d_i)]e^{\lambda(\tau_1+\tau_2)} - \tau_2 DC}{(DBe^{\lambda\tau_2} + DC)\lambda} - \frac{\tau_1}{\lambda}.$$

Notice that at $\lambda = i\omega$,

$$\begin{aligned}
&\operatorname{sign}\Big\{\frac{d\mathrm{Re}(\lambda)}{d\tau_1}\Big\} = \operatorname{sign}\Big\{\mathrm{Re}\Big(\Big(\frac{d\lambda}{d\tau_1}\Big)^{-1}\Big)\Big\} \\
&= \operatorname{sign}\Big\{\mathrm{Re}\Big(\frac{(i(A + d_i) - 2\omega)(\cos\omega(\tau_1 + \tau_2) + i\sin\omega(\tau_1 + \tau_2)) - \tau_2 DCi}{-(DB\cos\omega\tau_2 + iDB\sin\omega\tau_2)\omega}\Big)\Big\} \\
&= \operatorname{sign}\Big\{(DB\cos\omega\tau_2 + DC)2\omega\cos\omega(\tau_1 + \tau_2) + DB\sin\omega\tau_2(2\omega\sin\omega(\tau_1 + \tau_2) + \tau_2 DC) \\
&\qquad + DB(A + d_i)\sin\omega\tau_1\Big\} = 1.
\end{aligned}$$

Appendix E. Proof of Proposition 5.9. Similar to the proof of Proposition 5.8 in Appendix D, assume $\tau_1 + \tau_2 < \frac{\pi}{2\hat{\omega}}$. From (4.3), we have

$$\Big[2\lambda + (A + d_i) - \tau_1 DBe^{\lambda\tau_1} - DC(\tau_1 + \tau_2)e^{-\lambda(\tau_1+\tau_2)}\Big]\frac{d\lambda}{d\tau_2} = DC\lambda e^{-\lambda(\tau_1+\tau_2)}.$$

If $\lambda(\bar{\tau}_2) = i\omega$ is a root of (4.3) for some $\bar{\tau}_2 > 0$ with $\omega > 0$, then it must be simple. Otherwise, $\frac{d\lambda}{d\tau_2}\big|_{\tau_2=\bar{\tau}_2} = 0$ and leads to a contradiction, $DC\omega\cos\tau_1 + \bar{\tau}_2 = 0$. We show that if a root of (4.3) crosses the imaginary axis while τ_2 increases, it must cross from left to right. Obviously,

$$\Big(\frac{d\lambda}{d\tau_2}\Big)^{-1} = \frac{(2\lambda + (A + d_i))e^{\lambda(\tau_1+\tau_2)} - \tau_1 DBe^{-\lambda\tau_2}}{DC\lambda} - \frac{\tau_1 + \tau_2}{\lambda}.$$

Thus, at $\lambda = i\omega$,

$$\Big(\frac{d\lambda}{d\tau_2}\Big)^{-1} = \frac{2\omega\cos\omega(\tau_1 + \tau_2) + (A + d_i)\sin\omega(\tau_1 + \tau_2) - \tau_1 DB\sin\omega\tau_2}{DC\omega}.$$

Then, if $\tau_1 DB < A + d_i$,

$$\begin{aligned}
&\operatorname{sign}\Big\{\frac{d\mathrm{Re}(\lambda)}{d\tau_2}\Big\} = \operatorname{sign}\Big\{\mathrm{Re}\Big(\Big(\frac{d\lambda}{d\tau_2}\Big)^{-1}\Big)\Big\} \\
&= \operatorname{sign}\Big\{2\omega\cos\omega(\tau_1 + \tau_2) + (A + d_i)\sin\omega(\tau_1 + \tau_2) - \tau_1 DB\sin\omega\tau_2\Big\} = 1.
\end{aligned}$$

Acknowledgments. We would like to thank the referees and the associate editor for their valuable suggestions that enabled us to improve the presentation of this paper. The first author thanks Prof. Carlos Castillo-Chavez for his encouragement for the analysis of the characteristic equation when $\tau_1\tau_2 > 0$.

REFERENCES

[1] B. Ahrén and G. J. Taborsky Jr., *B-cell function and insulin secretion*, in Ellenberg and Rifkin's Diabetes Mellitus, 6th ed., D. Porte, R. S. Sherwin, and A. Baron, eds., McGraw-Hill Professional, Chapter 4, pp. 43–65.

[2] D. L. Bennette and S. A. Gourley, *Asymptotic properties of a delay differential equation model for the interaction of glucose with the plasma and interstitial insulin*, Appl. Math. Comput., 151 (2004), pp. 189–207.
[3] R. N. Bergman, *Pathogenesis and prediction of diabetes mellitus: Lessons from integrative physiology*, Irving L. Schwartz Lecture, Mount Sinai J. Medicine, 60 (2002), pp. 280–290.
[4] R. N. Bergman, D. T. Finegood, and S. E. Kahn, *The evolution of beta-cell dysfunction and insulin resistance in type* 2 *diabetes*, Eur. J. Clin. Invest., 32 (Suppl. 3) (2002), pp. 35–45.
[5] V. W. Bolie, *Coefficients of normal blood glucose regulation*, J. Appl. Physiol., 16 (1961), pp. 783–788.
[6] A. D. Cherrington, D. Sindelar, D. Edgerton, K. Steiner, and O. P. McGuinness, *Physiological consequences of phasic insulin release in the normal animal*, Diabetes, 51 (Suppl. 1) (2002), pp. S103–S108.
[7] J. B. Conway, *Functions of One Complex Variable*, 2nd ed., Springer-Verlag, New York, 1973; corrected fourth printing, 1986.
[8] K. L. Cooke and P. van den Driessche, *On zeroes of some transcendental equations*, Funkcial. Ekvac., 29 (1986), pp. 77–90.
[9] A. De Gaetano and O. Arino, *Mathematical modeling of the intravenous glucose tolerance test*, J. Math. Biol., 40 (2000), pp. 136–168.
[10] M. Derouich and A. Boutayeb, *The effect of physical exercise on the dynamics of glucose and insulin*, J. Biomechanics, 35 (2002), pp. 911–917.
[11] W. C. Duckworth, R. G. Bennett, and F. G. Hamel, *Insulin degradation: Progress and potential*, Endocr. Rev., 19 (1998), pp. 698–624.
[12] W. M. Hirsch, H. Hanish, and J.-P. Gabriel, *Differential equation model of some parasitic infections: Methods for the study of asymptotic behavior*, Comm. Pure. Appl. Math., 38 (1985), pp. 733–753.
[13] J. Keener and J. Sneyd, *Mathematical Physiology*, Springer-Verlag, New York, 1998.
[14] W. C. Knowler, P. H. Bennett, R. F. Hamman, and M. Miller, *Diabetes incidence and prevalence in Pima Indians: A* 19*-fold greater incidence than in Rochester, Minnesota*, Am. J. Epidemiol., 108 (1978), pp. 497–505.
[15] Y. Kuang, *Delay Differential Equations with Applications in Population Dynamics*, Math. Sci. Eng. 191, Academic Press, Boston, 1993.
[16] J. Li, Y. Kuang, and B. Li, *Analysis of IVGTT glucose-insulin interaction models with time delay*, Discrete Contin. Dyn. Syst. Ser. B, 1 (2001), pp. 103–124.
[17] J. Li, Y. Kuang, and C. Mason, *Modeling the glucose-insulin regulatory system and ultradian insulin secretory oscillations with two time delays*, J. Theoret. Biol., 242 (2006), pp. 722–735.
[18] A. Makroglou, J. Li, and Y. Kuang, *Mathematical models and software tools for the glucose-insulin regulatory system and diabetes: An overview*, Appl. Numer. Math., 56 (2006), pp. 559–573.
[19] A. Mukhopadhyay, A. De Gaetano, and O. Arino, *Modeling the intra-venous glucose tolerance test: A global study for a single-distributed-delay model*, Discrete Contin. Dyn. Syst. Ser. B, 4 (2004), pp. 407–417.
[20] N. Pørksen, M. Hollingdal, C. Juhl, P. Butler, J. D. Veldhuis, and O. Schmitz, *Pulsatile insulin secretion: Detection, regulation, and role in diabetes*, Diabetes, 51 (2002), pp. S245–S254.
[21] R. Prager, P. Wallace, and J. M. Olefsky, *In vivo kinetics of insulin action on peripheral glucose disposal and hepatic glucose output in normal and obese subjects*, J. Clin. Invest., 78 (1986), pp. 472–481.
[22] L. F. Shampine and S. Thompson, *Solving DDEs in MATLAB*, Appl. Numer. Math., 37 (2001), pp. 441–458; http://www.radford.edu/∼thompson.
[23] C. Simon and G. Brandenberger, *Ultradian oscillations of insulin secretion in humans*, Diabetes, 51 (2002), pp. S258–S261.
[24] J. Sturis, *Possible Mechanisms Underlying Slow Oscillations of Human Insulin Secretion*, Ph.D. thesis, The Technical University of Denmark, Lyngby, Denmark, 1991.
[25] J. Sturis, K. S. Polonsky, E. Mosekilde, and E. Van Cauter, *Computer model for mechanisms underlying ultradian oscillations of insulin and glucose*, Am. J. Physiol., 260 (1991), pp. E801–E809.
[26] I. M. Tolic, E. Mosekilde, and J. Sturis, *Modeling the insulin-glucose feedback system: The significance of pulsatile insulin secretion*, J. Theoret. Biol., 207 (2000), pp. 361–375.
[27] B. Topp, K. Promislow, G. De Vries, R. M. Miura, and D. T. Finegood, *A model of β-cell mass, insulin, and glucose kinetics: Pathways to diabetes*, J. Theoret. Biol., 206 (2000), pp. 605–619.